Research Square

Preprints are preliminary reports that have not undergone peer review.
They should not be considered conclusive, used to inform clinical practice,
or referenced by the media as validated information.

Prognostic value of the red blood cell distribution width-to-albumin ratio for in-hospital mortality in critically ill hypertensive patients with chronic kidney disease: a dual-center retrospective cohort study and machine learning analysis

Fan Zou
Third Affiliated Hospital of Sun Yat-sen University
Chengjiang Peng
Third Affiliated Hospital of Sun Yat-sen University
Xiuying Xiang
First Affiliated Hospital of Jinan University
Shaohong Ma
mashh6@mail.sysu.edu.cn

Third Affiliated Hospital of Sun Yat-sen University

Research Article

Keywords: Hypertensive heart disease with chronic kidney disease, Red blood cell distribution width-to-albumin ratio, Dual-center retrospective cohort study, Machine learning, Risk prediction model

Posted Date: November 23rd, 2026

DOI: https://doi.org/10.21203/rs.3.rs-11339566/v1

License: This work is licensed under a Creative Commons Attribution 4.0 International License.
Read Full License

Additional Declarations: No competing interests reported.

Prognostic value of the red blood cell distribution width-to-albumin ratio for in-hospital mortality in critically ill hypertensive patients with chronic kidney disease: a dual-center retrospective cohort study and machine learning analysis

Fan Zou[1]†, Chengjiang Peng[1]†, Xiuying Xiang[2]†, Shaohong Ma[1]*

[1] Department of Cardiovascular Surgery, The Third Affiliated Hospital of Sun Yat-sen University, Guangzhou 510630, Guangdong, China

[2] Department of Hematopathology, The First Affiliated Hospital of Jinan University, Guangzhou 510632, Guangdong, China

Correspondence: Shaohong Ma, Department of Cardiovascular Surgery, The Third Affiliated Hospital, Sun Yat-sen University, No. 600 Tianhe Road, Tianhe District, Guangzhou 510630, Guangdong, China. E-mail: mashh6@mail.sysu.edu.cn

†These authors contributed equally to this work.

Abstract

Background: The simultaneous presence of hypertensive heart disease and chronic kidney disease (HP+CKD) creates a uniquely vulnerable ICU phenotype, yet dedicated outcome-prediction tools for this population remain lacking. We therefore evaluated whether admission red blood cell distribution width-to-albumin ratio (RAR)—a ratio derived from two routine laboratory parameters—could independently predict in-hospital death in HP+CKD patients, and whether it adds discriminative value beyond established ICU severity instruments and its individual components.

Methods: We conducted a dual-center retrospective cohort study utilizing the MIMIC-IV database (2008–2014) for model development and the Third Affiliated Hospital of Sun Yat-sen University (SYSU; 2012–2025) for external validation. Our analytical framework integrated traditional regression with machine-learning approaches: we used multivariable logistic regression for effect estimation, restricted cubic splines for nonlinearity assessment, and a combination of LASSO plus Boruta for data-driven feature selection. Seven classifiers were benchmarked, and SHapley Additive exPlanations (SHAP) values were computed to interpret the final model.

Results: Our analysis included 1,865 patients from MIMIC-IV and 998 from SYSU, revealing in-hospital mortality rates of 21.5% and 12.4%, respectively. Across both cohorts, mortality rose monotonically across RAR quartiles, with the top quartile carrying 2.7- to 3.6-fold greater risk than the bottom quartile after full adjustment. The logistic regression model achieved area under the curve (AUC) values of 0.758 and 0.777 across the two cohorts, demonstrating strong calibration and net benefit.

Conclusions: RAR emerges as a robust, independent predictor of in-hospital mortality in critically ill HP+CKD patients, suggesting that its integration into routine risk assessments could enhance early identification of high-risk individuals.

Keywords: Hypertensive heart disease with chronic kidney disease; Red blood cell distribution width-to-albumin ratio; Dual-center retrospective cohort study; Machine learning; Risk prediction model

Background

Hypertensive heart disease complicated by chronic kidney disease (HP+CKD) imposes a compounded hemodynamic and metabolic burden: left ventricular pressure overload synergizes with uremic toxicity and volume dysregulation, collectively amplifying cardiovascular mortality beyond either condition alone [1,2]. When these patients require intensive care, their prognosis is further complicated by concurrent cardiac decompensation, inflammatory cascades, and catabolic states that standard ICU metrics may not fully capture [3,4]. Established ICU scoring instruments—SOFA and SAPS II—prioritize acute physiological derangements but exclude hematologic and nutritional parameters that may carry particular prognostic weight in HP+CKD, where chronic inflammation and protein-energy wasting are the rule rather than the exception [5,6]. Therefore, identifying simple, accessible predictors of in-hospital mortality in this population is clinically important.

In CKD, erythropoietic disruption and chronic oxidative stress widen the distribution of red cell volumes (RDW) [7], while concurrent nutritional depletion and hepatic synthetic impairment lower serum albumin [8]—two routinely measured parameters that, despite indexing distinct pathophysiological axes, have rarely been examined in combination in the ICU setting. The ratio of RDW to albumin (RAR) was first shown to correlate with CKD prevalence in the general population [9] and subsequently demonstrated superior prognostic accuracy over RDW alone for renal disease progression and mortality in CKD cohorts [10,11]. Beyond CKD, accumulating evidence links elevated RAR to adverse outcomes across diverse critical conditions, including sepsis [12], hepatic steatosis [13], arrhythmia [14], post-cardiac arrest [15], and acute decompensated heart failure [16]. Nevertheless, the existing literature is predominantly single-center with modest sample sizes [17,18], and no study has specifically examined whether RAR retains its prognostic utility in the HP+CKD subgroup or identified potential threshold effects that could guide clinical decision-making. Related haematological indices and risk-factor models have been evaluated in other acute settings—such as the RDW-to-platelet count ratio in paediatric sepsis [19] and mortality risk-factor analyses in patients with COVID-19 [20]—but not in patients with concurrent hypertensive heart disease

and CKD. For this high-risk subgroup of patients with HP+CKD, the dose-response relationship and threshold effects between RAR and in-hospital mortality remain insufficiently characterized.

We designed a two-stage investigation to fill this evidence gap. Model development employed the MIMIC-IV database (2008–2014), with independent external validation using electronic health records from the Third Affiliated Hospital of Sun Yat-sen University (2012–2025). Our analytic plan comprised three tiers: (i) multivariable regression to quantify the RAR–mortality association; (ii) restricted cubic spline modeling to detect nonlinearity and thresholds; and (iii) machine-learning-based feature selection to test the robustness of RAR against its individual components.

Methods

Study design and setting

We conducted a two-center, retrospective cohort analysis. The model derivation sample was extracted from MIMIC-IV (version 2.2, admissions 2008–2014); the independent validation sample was drawn from the clinical data warehouse of the Third Affiliated Hospital of Sun Yat-sen University (admissions 2012–2025). Both cohorts were assembled using identical eligibility criteria to ensure comparability. The study workflow is shown in Figure 1.

Figure 1. Study design flowchart of RAR and in-hospital mortality in critically ill patients with hypertensive heart disease and chronic kidney disease.

Participants and data sources

Adults (age ≥18 years) admitted to an ICU with ICD-9 or ICD-10 (40400, 40401, 40402, 40403, 40410, 40411, 40412, 40413, 40493, I130, I1310, I1311) codes indicating concurrent hypertensive heart disease and CKD were eligible. From each patient record, only the initial ICU admission was retained; encounters shorter than 3 hours or lacking first-day RDW or albumin measurements were removed. Access to MIMIC-IV was granted after the lead investigator (Xiuying Xiang) completed the CITI Program training and

executed the PhysioNet data-use agreement (credential ID: 67903425). For the SYSU cohort, all data were extracted from the institutional Big Data Center via a de-identified enterprise master patient index, with no direct patient identifiers accessible to the analytic team. After exclusions, 1,865 patients from MIMIC-IV and 998 patients from SYSU were included and grouped into RAR quartiles (Q1–Q4). The primary outcome was in-hospital mortality.

Exposure variable and covariates

RAR was computed by dividing RDW (expressed as a percentage) by serum albumin (g/dL) from the first laboratory panel obtained after ICU admission. We deliberately used initial values to capture the patients' baseline status prior to therapeutic interventions that could alter erythropoietic or nutritional parameters. The covariate set spanned five domains: (1) demographics (age, sex, race); (2) admission vital signs; (3) pharmacologic and device-based interventions (vasopressors, antiplatelet/anticoagulant agents, statins, mechanical ventilation, CRRT); (4) comorbidities (Charlson index); and (5) laboratory and severity measures (SOFA, APS III, SIRS, SAPS II, OASIS, Glasgow Coma Scale).

Missing data

Prior to analysis, variables exceeding 20% missingness were dropped. For the remaining incomplete variables, we applied multiple imputation via the mice package (R 4.4.1), generating five imputed datasets (m = 5) using random-forest-based imputation models. Pooled estimates were derived using Rubin rules.

Statistical and machine learning analysis

Distributional normality was assessed with the Shapiro-Wilk test. Accordingly, normally distributed continuous variables were presented as mean ± SD and evaluated via independent-samples t-tests, whereas skewed variables were reported as median (IQR) and analyzed with the Mann-Whitney U test. Categorical data were tabulated as counts (%) and compared via the chi-square test, with Fisher's exact test substituted when any expected cell count fell below five.

The RAR–mortality association was estimated through a hierarchical logistic regression strategy: (i) a crude model with RAR as the sole predictor; (ii) a demographic-adjusted model adding age, sex, and race; and (iii) a comprehensively adjusted model incorporating all covariates that achieved $P < 0.05$ in univariate screening. This tiered approach allowed us to quantify the degree of confounding attenuation at each level of adjustment. In the SYSU cohort, white blood cell count was excluded from Model 3 because of collinearity with RAR. Predictive performance was assessed using receiver operating characteristic curves and the area under the curve (AUC).

To visualize and test for non-linearity in the RAR–mortality relationship, we fitted restricted cubic spline functions with four knots at the 5th, 35th, 65th, and 95th percentile positions of the RAR distribution. The cohort-specific median served as the reference for odds ratio estimation. Segmental regression was then applied to identify the inflection point where the slope of the dose-response curve changed significantly. To assess the consistency of the RAR effect across clinically relevant subgroups (stratified by age, sex, race, vasopressor use, and CRRT status), we performed interaction analyses.

Feature selection employed two complementary algorithms: LASSO regression with 10-fold cross-validation (using the one-standard-error rule for penalty selection) and the Boruta wrapper method (100 iterations, $P < 0.05$ as the importance threshold). Seven classifiers were then trained and benchmarked: penalized logistic regression (glmnet), a single decision tree (rpart), random forest (500 trees), gradient-boosted trees via XGBoost and LightGBM (learning rate = 0.05, 200 rounds), a support vector machine with radial basis function kernel (e1071), and a feed-forward neural network with one hidden layer (nnet, size = 10). Model interpretability was enhanced through SHAP (SHapley Additive exPlanations) analysis, which quantified both global feature importance and individual-level risk attribution. Statistical computations were executed in R 4.4.1, with two-tailed P values below 0.05 deemed significant unless otherwise specified for multiplicity-adjusted analyses.

Results

Participant flow and baseline characteristics

Application of all eligibility filters yielded a final analytic sample of 1,865 MIMIC-IV patients and 998 SYSU patients. Table 1 summarizes their baseline characteristics, stratified by in-hospital survival status. In the MIMIC-IV cohort, overall in-hospital mortality was 21.5% (401/1,865). Non-survivors were older, had lower body weight, higher heart rate, and more frequent use of vasoactive agents. They also had higher RDW, RAR, severity scores (SOFA, OASIS, SAPS II, LODS, and SIRS), BUN, glucose, anion gap, prothrombin time, PTT, and INR, and lower albumin, red blood cell count, and chloride. Mechanical ventilation, CRRT, delirium, and malignancy were more common in non-survivors (all $P < 0.05$). A clear dose-response pattern emerged when mortality was examined by RAR quartile: rates climbed from 14.7% in Q1 to 39.7% in Q4 (Q2: 20.0%; Q3: 25.7%; P for trend < 0.001).

In the SYSU validation cohort, overall in-hospital mortality was 12.4% (124/998). RAR was significantly higher in non-survivors (6.47 ± 2.35 vs. 5.71 ± 1.76; $P < 0.001$), accompanied by higher RDW and lower albumin. Non-survivors also had higher white blood cell count, MCV, glucose, alkaline phosphatase, norepinephrine use, mechanical ventilation rate, and SOFA and OASIS scores, as well as lower calcium. Mortality differed significantly across RAR quartiles and was highest in Q4 (Q1, 21.0%; Q2, 14.5%; Q3, 27.4%; Q4, 37.1%; P = 0.001).

Table 1. Baseline characteristics of critically ill patients with hypertensive heart disease complicated by chronic kidney disease, stratified by in-hospital survival status

Variable	**MIMIC-IV: Overall**	**MIMIC-IV: Survival**	**MIMIC-IV: Death**	**P value**	**SYSU: Overall**	**SYSU: Survival**	**SYSU: Death**	**P value**
Demographics								
Male sex, n (%)	1,171 (62.8)	914 (62.4)	257 (64.1)	0.582	428 (42.9)	377 (43.1)	51 (41.1)	0.745

Variable	MIMIC-IV: Overall	MIMIC-IV: Survival	MIMIC-IV: Death	P value	SYSU: Overall	SYSU: Survival	SYSU: Death	P value
Weight, kg	87.74 ± 25.51	88.53 ± 25.78	84.84 ± 24.32	0.010	87.03 ± 27.92	86.66 ± 26.51	89.64 ± 36.38	0.266
Vital signs and haemodynamic parameters								
Respiratory rate, breaths/min	20.50 ± 6.22	20.27 ± 6.12	21.35 ± 6.48	0.002	—	—	—	—
SBP max, mmHg	156.87 ± 26.65	157.23 ± 25.69	155.54 ± 29.91	0.261	—	—	—	—
DBP max, mmHg	102.74 ± 25.40	102.98 ± 24.97	101.85 ± 26.96	0.433	—	—	—	—
MBP max, mmHg	122.67 ± 39.15	121.09 ± 35.85	128.44 ± 48.97	0.001	—	—	—	—
Haematological parameters								
Platelet count, $\times 10^9$/L	196.51 ± 99.96	197.09 ± 99.03	194.39 ± 103.39	0.632	195.44 ± 83.60	194.00 ± 80.89	205.64 ± 100.47	0.147
WBC count, $\times 10^9$/L	12.55 ± 9.37	12.15 ± 9.13	13.98 ± 10.08	0.001	11.03 ± 5.83	10.63 ± 5.47	13.89 ± 7.31	<0.001
Haematocrit, %	30.78 ± 6.68	30.87 ± 6.65	30.45 ± 6.81	0.262	31.54 ± 6.14	31.48 ± 6.12	31.95 ± 6.26	0.421
RBC count, $\times 10^{12}$/L	3.36 ± 0.78	3.38 ± 0.78	3.29 ± 0.79	0.042	3.51 ± 0.72	3.51 ± 0.72	3.52 ± 0.76	0.914

Variable	MIMIC-IV: Overall	MIMIC-IV: Survival	MIMIC-IV: Death	P value	SYSU: Overall	SYSU: Survival	SYSU: Death	P value
RDW, %	16.12 ± 2.61	15.93 ± 2.51	16.80 ± 2.83	<0.001	15.70 ± 2.33	15.62 ± 2.21	16.25 ± 3.01	0.005
MCV, fL	92.17 ± 7.62	91.89 ± 7.51	93.21 ± 7.95	0.002	90.18 ± 7.08	89.93 ± 6.90	91.95 ± 8.07	0.003
MCHC, g/dL	31.68 ± 1.60	31.70 ± 1.60	31.58 ± 1.63	0.175	32.72 ± 1.36	32.73 ± 1.35	32.60 ± 1.38	0.302
Serum biochemical parameters								
Creatinine, mg/dL	2.26 ± 1.42	2.20 ± 1.41	2.48 ± 1.45	0.001	2.91 ± 2.49	2.96 ± 2.57	2.61 ± 1.72	0.150
BUN, mg/dL	47.57 ± 29.09	45.37 ± 28.52	55.61 ± 29.76	<0.001	44.46 ± 26.71	44.40 ± 26.88	44.90 ± 25.63	0.846
Glucose, mg/dL	168.84 ± 93.16	166.40 ± 90.59	177.74 ± 101.61	0.031	156.05 ± 98.54	152.37 ± 94.39	182.05 ± 121.23	0.002
Calcium, mg/dL	8.57 ± 0.83	8.59 ± 0.81	8.50 ± 0.91	0.060	8.37 ± 0.85	8.39 ± 0.85	8.21 ± 0.85	0.028
Chloride, mEq/L	101.06 ± 7.13	101.35 ± 6.93	100.01 ± 7.72	0.001	104.71 ± 6.81	104.73 ± 6.70	104.56 ± 7.56	0.802
Potassium, mEq/L	4.48 ± 0.84	4.45 ± 0.82	4.57 ± 0.88	0.010	4.34 ± 0.84	4.32 ± 0.83	4.47 ± 0.91	0.067
Sodium, mEq/L	137.75 ± 5.79	137.88 ± 5.57	137.30 ± 6.53	0.076	138.52 ± 5.21	138.50 ± 5.22	138.65 ± 5.17	0.765

Variable	MIMIC-IV: Overall	MIMIC-IV: Survival	MIMIC-IV: Death	P value	SYSU: Overall	SYSU: Survival	SYSU: Death	P value
Anion gap, mEq/L	15.44 ± 4.82	15.07 ± 4.62	16.80 ± 5.30	<0.001	11.93 ± 4.64	11.85 ± 4.52	12.49 ± 5.42	0.156
Alkaline phosphatase, IU/L	96.32 ± 4.17	96.50 ± 3.92	95.66 ± 4.95	<0.001	94.31 ± 72.97	91.70 ± 62.20	112.71 ± 123.75	0.003
Coagulation parameters								
PTT, s	43.54 ± 30.37	42.56 ± 29.39	47.10 ± 33.49	0.008	—	—	—	—
INR	1.72 ± 1.04	1.67 ± 0.97	1.90 ± 1.24	<0.001	—	—	—	—
RAR index								
RAR quartile, n (%)	<0.001	0.001						
Q1 (lowest)	466 (25.0)	407 (27.8)	59 (14.7)	249 (24.9)	223 (25.5)	26 (21.0)		
Q2	466 (25.0)	386 (26.4)	80 (20.0)	249 (24.9)	231 (26.4)	18 (14.5)		
Q3	466 (25.0)	363 (24.8)	103 (25.7)	250 (25.1)	216 (24.7)	34 (27.4)		
Q4 (highest)	467 (25.0)	308 (21.0)	159 (39.7)	250 (25.1)	204 (23.3)	46 (37.1)		
Comorbidities								
Heart failure, n (%)	1,842 (98.8)	1,442 (98.5)	400 (99.8)	0.078	296 (29.7)	261 (29.9)	35 (28.2)	0.788
Peripheral vascular	389 (20.9)	306 (20.9)	83 (20.7)	0.984	1 (0.1)	0 (0.0)	1 (0.8)	0.254

Variable	MIMIC-IV: Overall	MIMIC-IV: Survival	MIMIC-IV: Death	P value	SYSU: Overall	SYSU: Survival	SYSU: Death	P value
disease, n (%)								
Myocardial infarction, n (%)	752 (40.3)	575 (39.3)	177 (44.1)	0.089	—	—	—	—
Cerebrovascular disease, n (%)	283 (15.2)	210 (14.3)	73 (18.2)	0.067	—	—	—	—
Malignant cancer, n (%)	207 (11.1)	148 (10.1)	59 (14.7)	0.012	—	—	—	—
ICU interventions								
Epinephrine, n (%)	163 (8.7)	111 (7.6)	52 (13.0)	0.001	6 (0.6)	6 (0.7)	0 (0.0)	0.761
Dobutamine, n (%)	125 (6.7)	70 (4.8)	55 (13.7)	<0.001	—	—	—	—
Dopamine, n (%)	75 (4.0)	42 (2.9)	33 (8.2)	<0.001	—	—	—	—
Milrinone, n (%)	54 (2.9)	45 (3.1)	9 (2.2)	0.478	—	—	—	—
Mechanical ventilation, n (%)	1,501 (80.5)	1,158 (79.1)	343 (85.5)	0.005	298 (29.9)	226 (25.9)	72 (58.1)	<0.001
CRRT, n (%)	177 (9.5)	81 (5.5)	96 (23.9)	<0.001	156 (15.6)	133 (15.2)	23 (18.5)	0.410
Illness severity scores								

Variable	MIMIC-IV: Overall	MIMIC-IV: Survival	MIMIC-IV: Death	P value	SYSU: Overall	SYSU: Survival	SYSU: Death	P value
SOFA score	6.59 ± 3.53	5.93 ± 3.12	8.98 ± 3.87	<0.001	7.06 ± 3.62	6.74 ± 3.51	9.27 ± 3.61	<0.001
SIRS score	2.43 ± 0.90	2.35 ± 0.89	2.71 ± 0.89	<0.001	—	—	—	—
LODS score	6.21 ± 2.82	5.73 ± 2.58	7.95 ± 2.97	<0.001	—	—	—	—
SAPSII score	43.60 ± 13.22	41.34 ± 11.82	51.89 ± 14.71	<0.001	—	—	—	—
GCS score	14.38 ± 1.90	14.42 ± 1.89	14.25 ± 1.96	0.122	—	—	—	—
Other clinical parameters								
Urine output, mL	1,993.81 ± 1,668.83	2,124.74 ± 1,705.61	1,515.81 ± 1,430.46	<0.001	16,088.56 ± 48,052.89	15,695.26 ± 49,942.79	18,860.69 ± 31,694.30	0.493

Note: Continuous variables are presented as mean ± standard deviation; categorical variables as n (%). P values were derived from Student's t-test or Mann–Whitney U test for continuous variables and chi-square test or Fisher's exact test for categorical variables. Bold P values indicate statistical significance ($P < 0.05$). "—" indicates variables not available in the corresponding cohort database.

Multivariable logistic regression analysis

Twelve variables retained independent prognostic significance in the MIMIC-IV multivariable model, whereas seven emerged in the SYSU model (Table 2). In MIMIC-IV, higher age, dobutamine use, BUN, SOFA score, SIRS score, LODS score, and CRRT were associated with increased mortality, whereas

norepinephrine use, higher creatinine, and higher chloride were associated with lower mortality. In SYSU, MCV, mechanical ventilation, SOFA score, OASIS score, alkaline phosphatase, and glucose were independently predictive. A critical observation was that neither RDW nor albumin achieved statistical significance when modeled as individual predictors in either cohort, whereas RAR retained robust independent associations—indicating that the ratio captures synergistic information lost when its components are considered in isolation.

Table 2. Multivariable logistic regression analysis of factors associated with in-hospital mortality in critically ill patients with hypertensive heart disease complicated by chronic kidney disease

Variable	**MIMIC-IV: OR**	**MIMIC-IV: 95% CI**	**MIMIC-IV: P**	**SYSU: OR**	**SYSU: 95% CI**	**SYSU: P**
Age	1.04	1.02–1.05	<0.001	—	—	—
Delirium	0.97	0.71–1.33	0.846	—	—	—
Liquid output	1.00	1.00–1.00	0.001	—	—	—
Dobutamine use	1.84	1.12–3.03	0.017	—	—	—
Dopamine use	1.57	0.85–2.91	0.151	—	—	—
Epinephrine use	0.65	0.39–1.09	0.100	—	—	—
Norepinephrine use	0.62	0.43–0.90	0.011	2.31	0.99–5.39	0.053
PT	1.23	0.89–1.70	0.215	—	—	—
aPTT	1.00	1.00–1.01	0.072	—	—	—
INR	0.10	0.00–3.56	0.208	—	—	—
Creatinine	0.74	0.63–0.86	<0.001	—	—	—
Chloride	0.96	0.94–0.98	<0.001	—	—	—
Potassium	0.90	0.76–1.07	0.243	—	—	—

Variable	MIMIC-IV: OR	MIMIC-IV: 95% CI	MIMIC-IV: P	SYSU: OR	SYSU: 95% CI	SYSU: P
Anion gap	1.00	0.97–1.04	0.773	—	—	—
BUN	1.01	1.00–1.02	0.005	—	—	—
WBC	1.00	0.99–1.01	0.762	1.06	1.03–1.09	<0.001
RDW	0.99	0.83–1.18	0.924	1.13	0.92–1.40	0.241
MCV	1.01	0.99–1.03	0.311	1.05	1.02–1.08	<0.001
Albumin	1.00	0.34–2.89	0.996	0.59	0.15–2.31	0.453
Weight	1.00	0.99–1.01	0.809	—	—	—
Heart rate	1.00	0.99–1.01	0.797	—	—	—
Respiratory rate	1.02	0.99–1.04	0.144	—	—	—
Alkaline phosphatase	0.96	0.93–0.99	0.017	1.00	1.00–1.00	0.044
Mechanical ventilation	1.04	0.71–1.54	0.828	2.05	1.28–3.28	0.003
Malignant cancer	1.48	0.97–2.26	0.070	—	—	—
SIRS score	1.32	1.10–1.58	0.003	—	—	—
LODS score	1.13	1.04–1.22	0.004	—	—	—
OASIS score	0.99	0.96–1.01	0.247	1.03	1.00–1.06	0.026
SAPSII score	1.00	0.98–1.02	0.807	—	—	—
SOFA score	1.25	1.17–1.34	<0.001	1.09	1.02–1.17	0.012
CRRT use	2.34	1.47–3.73	<0.001	—	—	—
Maximum MBP	1.00	1.00–1.00	0.943	—	—	—

Variable	MIMIC-IV: OR	MIMIC-IV: 95% CI	MIMIC-IV: P	SYSU: OR	SYSU: 95% CI	SYSU: P
Calcium	—	—	—	1.03	0.79–1.33	0.823
Glucose	—	—	—	1.00	1.00–1.00	0.044

Note: Odds ratios (OR) with 95% confidence intervals (CI) were derived from multivariable logistic regression with in-hospital mortality as the dependent variable. P < 0.05 indicates statistical significance, and significant P values are shown in bold. "—" indicates that the variable was not entered into the corresponding cohort model.

†Variables entered into the MIMIC-IV model: age, delirium, liquid output, vasoactive medications (dobutamine, dopamine, epinephrine, norepinephrine), coagulation parameters (PT, aPTT, INR), laboratory indices (creatinine, chloride, potassium, anion gap, BUN, WBC, RDW, MCV, albumin, alkaline phosphatase), clinical parameters (weight, heart rate, respiratory rate, maximum MBP), treatment indicators (mechanical ventilation, CRRT), comorbidities (malignant cancer), and disease severity scores (SIRS, LODS, OASIS, SAPSII, SOFA).

‡Variables entered into the SYSU model: WBC, MCV, alkaline phosphatase, glucose, mechanical ventilation, OASIS score, and SOFA score. White blood cell count was excluded because of collinearity with RAR.

§RDW and albumin—the individual components of the RAR index—were not independently significant in either cohort, supporting the rationale for using the composite RAR index.

Association between RAR and in-hospital mortality

Referenced to Q1, the top RAR quartile (Q4) showed a strong and progressively attenuated mortality association: the crude OR of 6.15 (95% CI, 4.33–8.72) in MIMIC-IV was reduced to 3.56 (2.45–5.17) after demographic adjustment and to 2.73 (1.85–4.05) in the fully adjusted model, with a consistent trend across quartiles (P for trend < 0.001); the trend-test OR was 1.23 (95% CI, 1.15–1.31; P < 0.001). In the SYSU cohort, the corresponding ORs were 2.06 (95% CI, 1.34–3.17), 1.93 (95% CI, 1.22–3.05), and 1.85 (95% CI, 1.06–3.28), with a trend-test OR of 1.21 (95% CI, 1.04–1.40; P = 0.013). RAR remained significant in

the fully adjusted model, whereas RDW and albumin did not when entered individually (Table 3).

Table 3. Association between red blood cell distribution width-to-albumin ratio (RAR) quartiles and in-hospital mortality in critically ill patients with hypertensive heart disease complicated by chronic kidney disease

Exposure	**Model 1: OR (95% CI)**	**Model 1: P**	**Model 2: OR (95% CI)**	**Model 2: P**	**Model 3: OR (95% CI)**	**Model 3: P**
MIMIC-IV cohort (n = 1,865)						
Q1 (lowest)	1.00 (Reference)	1.00 (Reference)	1.00 (Reference)			
Q2	1.43 [1.00, 2.06]	0.054	1.41 [0.98, 2.04]	0.068	1.11 [0.74, 1.69]	0.610
Q3	1.96 [1.38, 2.79]	<0.001	1.96 [1.38, 2.81]	<0.001	1.43 [0.96, 2.13]	0.082
Q4 (highest)	3.56 [2.56, 5.00]	<0.001	3.69 [2.65, 5.21]	<0.001	2.73 [1.87, 4.02]	<0.001
P for trend	1.49 [1.36, 1.65]	<0.001	1.52 [1.38, 1.67]	<0.001	1.41 [1.26, 1.58]	<0.001
SYSU cohort (n = 998)						
Q1 (lowest)	1.00 (Reference)	1.00 (Reference)	1.00 (Reference)			
Q2	0.67 [0.35, 1.25]	0.209	0.66 [0.34, 1.22]	0.189	0.59 [0.30, 1.13]	0.114
Q3	1.35 [0.79, 2.34]	0.279	1.36 [0.79, 2.36]	0.271	1.26 [0.71, 2.28]	0.432

Exposure	Model 1: OR (95% CI)	Model 1: P	Model 2: OR (95% CI)	Model 2: P	Model 3: OR (95% CI)	Model 3: P
Q4 (highest)	1.93 [1.16, 3.28]	0.012	1.95 [1.17, 3.32]	0.011	1.85 [1.06, 3.28]	0.032
P for trend	1.26 [1.10, 1.44]	0.001	1.27 [1.11, 1.45]	0.001	1.21 [1.04, 1.40]	0.013

Note: Odds ratios (OR) with 95% confidence intervals (CI) were estimated by multivariable logistic regression with in-hospital mortality as the dependent variable. RAR was stratified into quartiles (Q1–Q4), with Q1 (lowest) as the reference group. P for trend was calculated by modelling the RAR quartile median as a continuous variable. Significant P values (< 0.05) are shown in bold.

Model specifications: Model 1, crude (unadjusted); Model 2, adjusted for age, sex, and race; Model 3 (MIMIC-IV), adjusted for age, sex, SOFA score, liquid output, dobutamine, norepinephrine, creatinine, chloride, BUN, alkaline phosphatase, SIRS score, LODS score, and CRRT; Model 3 (SYSU), adjusted for SOFA score, glucose, age, sex, MCV, mechanical ventilation, alkaline phosphatase and OASIS score. White blood cell count was excluded from Model 3 because of collinearity with RAR.

Restricted cubic spline analysis

Spline modeling confirmed a positive monotonic trend between RAR and mortality risk in both cohorts, though the functional forms differed: the MIMIC-IV curve was approximately linear (Figure 2A), whereas the SYSU curve followed a J-shaped pattern (Figure 2B). In the MIMIC-IV cohort, the relationship was approximately linear and monotonically increasing, with the OR rising from 0.7 (95% CI, 0.4–1.2) at RAR approximately 3.8 to 2.9 (95% CI, 1.6–5.3) at RAR approximately 10.5; a threshold effect was observed at an RAR of approximately 5.0 (P for non-linearity < 0.001) (Figure 2A). In the SYSU cohort, the relationship was J-shaped, with a nadir at an RAR of approximately 5.0 (OR approximately 0.6) and risk increasing above RAR approximately 5.8–6.0: OR approximately 1.7 (95% CI, 1.0–2.8) at RAR approximately 7.5 and OR approximately 2.5 (95% CI, 1.0–5.8) at RAR approximately 12.5 (P for non-linearity < 0.001) (Figure 2B). Taken together, both cohorts indicate that mortality risk rises substantially

when RAR exceeds 5.0–6.0.

Figure 2. Restricted cubic spline (RCS) analysis of the association between RAR and in-hospital mortality. **(A)** RCS analysis in the MIMIC-IV derivation cohort (n = 1,865). The association between red cell distribution width-to-albumin ratio (RAR) and in-hospital mortality was modeled using restricted cubic splines with 4 knots, adjusted for age, dobutamine use, norepinephrine use, creatinine, chloride, blood urea nitrogen, alkaline phosphatase, SOFA score, SIRS score, LODS score, and CRRT use (Model 3). The reference point was set at the 25th percentile of RAR. The shaded area represents the 95% confidence interval. **(B)** RCS analysis in the Third Affiliated Hospital of Sun Yat-sen University (SYSU) validation cohort (n = 998). The same modeling approach was applied, adjusted for SOFA score, glucose, age, sex, MCV, mechanical ventilation, OASIS score (Model 3; white blood cell count was excluded due to collinearity with RAR). The reference point was set at the 25th percentile of RAR. Both panels demonstrate a non-linear association between RAR and in-hospital mortality, with increasing mortality risk at higher RAR values.

Subgroup and sensitivity analyses

Subgroup analyses showed that the positive association between RAR and in-hospital mortality was consistent across most predefined subgroups (Figure 3). In the MIMIC-IV cohort, the overall OR was 1.30 (95% CI, 1.20–1.41; $P < 0.001$), and the association remained robust across subgroups defined by age, sex, race, norepinephrine use, and CRRT; only the age subgroup showed a significant interaction ($P = 0.04$) (Figure 3A). In the SYSU cohort, the overall OR was 1.14 (95% CI, 1.03–1.25; $P = 0.008$), with a consistent direction across subgroups and no significant interactions (all $P > 0.14$) (Figure 3B).

Figure 3. Subgroup analysis of the association between RAR and in-hospital mortality. **(A)** Subgroup analysis in the MIMIC-IV derivation cohort (n = 1,865). Forest plots display the adjusted odds ratios (ORs) and 95% confidence intervals (CIs) for in-hospital mortality across predefined subgroups. The model was adjusted for age, dobutamine use, norepinephrine use, creatinine, chloride, blood urea nitrogen, alkaline phosphatase, SOFA score, SIRS score, LODS score, and CRRT use (Model 3). The size of the squares reflects the weight of each subgroup. The diamond represents the overall effect estimate. **(B)** Stratified

analysis in the Third Affiliated Hospital of Sun Yat-sen University (SYSU) validation cohort (n = 998). The same modeling approach was applied, adjusted for white blood cell count, mean corpuscular volume, mechanical ventilation, norepinephrine use, SOFA score, and OASIS score (Model 3; white blood cell count was excluded due to collinearity with RAR). Both panels demonstrate consistent associations between RAR and in-hospital mortality across major subgroups, with higher RAR values associated with increased mortality risk.

Machine learning feature selection

Both selection algorithms converged on RAR as a core predictor. In MIMIC-IV, LASSO (using the one-SE rule) shrank the feature set to five variables—RAR, SOFA, LODS, CRRT, and SAPS II—and Boruta independently confirmed this subset. Notably, the LASSO coefficient path showed RAR remaining non-zero across a broad penalty range, while RDW and albumin were penalized to zero at moderate lambda values, suggesting that the composite ratio subsumes the predictive information of its parts. In the SYSU cohort, LASSO retained RAR, SOFA score, and OASIS score, and the Boruta algorithm confirmed these and additional variables; RDW was rejected, and albumin was classified as tentative. These findings indicate that RAR is a non-redundant core predictor in both cohorts (Figure 4).

Figure 4. Machine learning feature selection for predicting in-hospital mortality in critically ill patients with hypertensive heart disease and chronic kidney disease. **(A)** LASSO coefficient paths in the MIMIC-IV cohort showing the trajectories of standardised regression coefficients as the penalty parameter λ (log scale) increases; variables with non-zero coefficients at the optimal λ (indicated by the vertical dashed line) were selected. **(B)** Ten-fold cross-validation error plot in the MIMIC-IV cohort showing the mean squared error (MSE) across the λ spectrum; the vertical dashed lines denote the λ value that minimises the MSE (left) and the largest λ within one standard error of the minimum (right). **(C)** Boruta feature importance plot in the MIMIC-IV cohort comparing the importance of each candidate variable (coloured bars) against the maximum importance of shadow features (grey boxes); green bars indicate confirmed features, red bars indicate rejected features, and blue bars indicate tentative features. **(D)** Consensus feature selection network diagram in the MIMIC-IV cohort illustrating the overlap between features identified by Boruta (green

nodes) and LASSO (orange nodes); the central hub (bold) denotes variables that were selected by both algorithms, supporting their robustness for subsequent multivariable model development. **(E)** LASSO coefficient paths in the SYSU cohort showing the trajectories of standardised regression coefficients as the penalty parameter λ (log scale) increases; variables with non-zero coefficients at the optimal λ (indicated by the vertical dashed line) were selected. **(F)** Ten-fold cross-validation error plot in the SYSU cohort showing the mean squared error (MSE) across the λ spectrum; the vertical dashed lines denote the λ value that minimises the MSE (left) and the largest λ within one standard error of the minimum (right). **(G)** Boruta feature importance plot in the SYSU cohort comparing the importance of each candidate variable (coloured bars) against the maximum importance of shadow features (grey boxes); green bars indicate confirmed features, red bars indicate rejected features, and blue bars indicate tentative features. **(H)** Consensus feature selection network diagram in the SYSU cohort illustrating the overlap between features identified by Boruta (green nodes) and LASSO (orange nodes); the central hub (bold) denotes variables that were selected by both algorithms, supporting their robustness for subsequent multivariable model development.

Machine learning model comparison and LR selection

On the MIMIC-IV held-out test set, logistic regression and SVM tied for the best discrimination (AUC = 0.758, 95% CI 0.722–0.793 each). The remaining models ranked as follows: ANN (0.755), XGBoost (0.745), LightGBM (0.725), random forest (0.717), and decision tree (0.677) (Figure 5A). Calibration curves confirmed good fit for LR, SVM, and ANN (Figure 5B), and decision-curve analysis demonstrated that these three models yielded the greatest net benefit across clinically relevant threshold probabilities (Figure 5C). Given that LR matched the top-performing algorithms while offering superior clinical interpretability—a prerequisite for bedside adoption—we designated it as the primary prediction model. In the SYSU validation cohort, LR achieved an AUC of 0.777, followed by XGBoost (0.776), LightGBM (0.759), ANN (0.750), random forest (0.738), decision tree (0.724), and SVM (0.674) (Figure 5D). LR, LightGBM, and XGBoost were well calibrated (Figure 5E), and decision curve analysis showed that LR, XGBoost, and LightGBM provided the highest clinical net benefit across threshold probabilities of 0.05–0.80 (Figure 5F). The LR model showed the smallest cross-cohort decline (ΔAUC = 0.019) and was

therefore selected as the primary clinical prediction model.

Figure 5. Comparative performance of seven machine learning models for predicting in-hospital mortality in critically ill patients with hypertensive heart disease and chronic kidney disease. **(A)** Receiver operating characteristic (ROC) curves in the MIMIC-IV cohort showing the trade-off between the true positive rate (sensitivity) and the false positive rate (1 − specificity) for each machine learning model; the area under the ROC curve (AUC) values are annotated in the legend, with the random classifier diagonal shown as a reference. **(B)** Calibration curves in the MIMIC-IV cohort plotting the observed true probability against the predicted probability for each model; the diagonal dashed line represents perfect calibration, and the deviation from this line indicates the degree of model miscalibration. **(C)** Decision curve analysis (DCA) in the MIMIC-IV cohort evaluating the net benefit of each model across a range of threshold probabilities; the horizontal dashed line (Treat None) and the grey diagonal line (Treat All) serve as reference strategies. **(D)** Receiver operating characteristic (ROC) curves in the SYSU cohort showing the trade-off between the true positive rate and the false positive rate for each machine learning model; the AUC values are annotated in the legend, with the random classifier diagonal shown as a reference. **(E)** Calibration curves in the SYSU cohort plotting the observed true probability against the predicted probability for each model; the diagonal dashed line represents perfect calibration, and the deviation from this line indicates the degree of model miscalibration. **(F)** Decision curve analysis (DCA) in the SYSU cohort evaluating the net benefit of each model across a range of threshold probabilities; the horizontal dashed line (Treat None) and the grey diagonal line (Treat All) serve as reference strategies.

LR performance and SHAP interpretability

In the MIMIC-IV training cohort, LR achieved an AUC of 0.780 (95% CI, 0.761–0.799), with minimal overfitting (training–test ΔAUC = 0.022) (Figure 6D). At the default threshold of 0.50, accuracy was 81.4%, specificity was 95.8%, sensitivity was 28.9%, positive predictive value was 65.2%, negative predictive value was 83.1%, and the F1 score was 40.1% (Figure 6A). Calibration was excellent at low-to-moderate probabilities (Figure 6C), and decision curve analysis showed positive net benefit across threshold probabilities of approximately 0.02–0.82 (Figure 6B).

In the SYSU validation cohort, LR achieved an AUC of 0.777 (95% CI, 0.748–0.806), consistent with the MIMIC-IV cohort (ΔAUC = 0.012) (Figure 6H). Calibration was satisfactory in the moderate-probability range (0.10–0.60) (Figure 6E), and decision curve analysis showed that the LR model outperformed treat-all and treat-none strategies across threshold probabilities of approximately 5%–85% (Figure 6G). At the default threshold of 0.50, accuracy was 87.6%, specificity was 98.97%, precision was 50.0%, and sensitivity was 7.26%; the low sensitivity reflected the low event rate (12.4%) and could be improved by lowering the threshold for screening (Figure 6F).

Figure 6. Performance of the final logistic regression (LR) model for predicting in-hospital mortality in critically ill patients with hypertensive heart disease and chronic kidney disease. **(A)** Confusion matrix for the LR model in the MIMIC-IV cohort (training set) showing the distribution of true negatives (TN = 1,402), false positives (FP = 62), false negatives (FN = 285), and true positives (TP = 116); actual labels are shown on the y-axis and predicted labels on the x-axis, with the colour bar indicating the corresponding cell counts. **(B)** Decision curve analysis (DCA) for the LR model in the MIMIC-IV cohort (training set) evaluating the net benefit across threshold probabilities; the horizontal dashed line (Treat None) and the diagonal line (Treat All) serve as reference strategies. **(C)** Calibration curve for the LR model in the MIMIC-IV cohort (training set) plotting the observed true probability against the predicted probability; the diagonal dashed line represents perfect calibration, and the deviation from this line indicates model miscalibration. **(D)** Receiver operating characteristic (ROC) curve for the LR model in the MIMIC-IV cohort (training set) showing the trade-off between the true positive rate and the false positive rate; the area under the ROC curve (AUC = 0.780) is annotated in the legend, with the random classifier diagonal shown as a reference. **(E)** Calibration curve for the LR model in the SYSU cohort (training set) plotting the observed true probability against the predicted probability; the diagonal dashed line represents perfect calibration, and the deviation from this line indicates model miscalibration. **(F)** Confusion matrix for the LR model in the SYSU cohort (training set) showing the distribution of true negatives (TN = 865), false positives (FP = 9), false negatives (FN = 115), and true positives (TP = 9); actual labels are shown on the y-axis and predicted labels on the x-axis, with the colour bar indicating the corresponding cell counts. **(G)** Decision curve analysis (DCA) for the LR model in the SYSU cohort (training set) evaluating the net benefit across threshold probabilities; the horizontal dashed line (Treat None) and the diagonal line (Treat

All) serve as reference strategies. **(H)** Receiver operating characteristic (ROC) curve for the LR model in the SYSU cohort (training set) showing the trade-off between the true positive rate and the false positive rate; the area under the ROC curve (AUC = 0.777) is annotated in the legend, with the random classifier diagonal shown as a reference.

In the SHAP global importance ranking for MIMIC-IV, RAR occupied the top position (mean |SHAP| = 0.06), surpassing SOFA (0.05), SAPS II (0.04), LODS (0.02), and CRRT (0.01) (Figure 7A). The corresponding dependence plot revealed a monotonic positive attribution: as RAR increased, its SHAP value rose steadily, consistently pushing the predicted mortality probability upward (Figure 7B). The SHAP hierarchy in SYSU differed: mechanical ventilation (0.024), SOFA (0.023), and OASIS (0.019) led the ranking, with RAR in the fifth position (0.017) (Figure 7C). Despite its lower rank, the RAR dependence plot maintained the same positive directional attribution observed in MIMIC-IV (Figure 7D), supporting the cross-cohort consistency of the RAR signal.

Figure 7. SHapley Additive exPlanations (SHAP) analysis of the logistic regression (LR) model for predicting in-hospital mortality in critically ill patients with hypertensive heart disease complicated by chronic kidney disease. **(A)** Mean SHAP feature importance bar chart in the MIMIC-IV cohort displaying the top six predictors ranked by their mean absolute SHAP values; the horizontal bars represent the mean |SHAP value| for each feature, with the numerical values annotated at the end of each bar. RAR exhibited the highest mean |SHAP value| (+0.06), followed by SOFA score (+0.05), SAPSII score (+0.04), LODS score (+0.02), CRRT (+0.01), and the constant term (+0). **(B)** SHAP beeswarm plot in the MIMIC-IV cohort illustrating the distribution of SHAP values for each feature across all patients; each dot represents a single patient, the horizontal position indicates the SHAP value (impact on model output), and the colour gradient from blue (low feature value) to red (high feature value) denotes the corresponding feature value. Positive SHAP values push the prediction toward higher mortality risk, while negative values push it toward lower risk. **(C)** Mean SHAP feature importance bar chart in the SYSU cohort displaying the top seven predictors ranked by their mean absolute SHAP values; the horizontal bars represent the mean |SHAP value| for each feature, with the numerical values annotated at the end of each bar. Mechanical ventilation (+0.02), SOFA score (+0.02), OASIS score (+0.02), white blood cell count (+0.02), and RAR (+0.02) showed comparable importance, followed by norepinephrine (+0) and the constant term (+0). **(D)**

SHAP beeswarm plot in the SYSU cohort illustrating the distribution of SHAP values for each feature across all patients; each dot represents a single patient, the horizontal position indicates the SHAP value (impact on model output), and the colour gradient from blue (low feature value) to red (high feature value) denotes the corresponding feature value. Positive SHAP values push the prediction toward higher mortality risk, while negative values push it toward lower risk.

Discussion

This dual-center investigation yielded three principal findings. First, admission RAR independently predicted in-hospital mortality in critically ill HP+CKD patients after comprehensive covariate adjustment, with the highest quartile conferring nearly three-fold excess risk relative to the lowest (adjusted OR 2.73 in MIMIC-IV; 1.85 in SYSU). Second, RAR demonstrated superior prognostic utility compared with its individual components—neither RDW nor albumin retained significance when modeled separately—suggesting that the ratio captures synergistic pathophysiological information. Third, machine-learning feature selection algorithms (LASSO and Boruta) consistently retained RAR while eliminating its components, and logistic regression achieved stable discrimination across cohorts (AUC 0.758–0.777) with minimal cross-site degradation.

The observation that RAR outperformed RDW and albumin as individual predictors aligns with the broader principle that ratio-based biomarkers can integrate complementary pathophysiological signals [19,21,22]. Whereas RDW alone is susceptible to confounding by iron deficiency or hemolysis, and albumin alone is influenced by hydration status and hepatic function, their ratio may provide a more stable composite signal of the inflammatory-nutritional axis. Indeed, both LASSO and Boruta analyses provided algorithm-independent confirmation: both approaches retained RAR while discarding its components, and Boruta explicitly rejected RDW in the validation cohort. Prior mediation analysis further indicated that RAR exerted a significant mediating effect on the relationship between the stress hyperglycemia ratio and mortality risk [23]. Thus, RAR captures synergistic prognostic information that single markers cannot provide.

The non-linear modeling revealed an informative between-cohort difference: while the MIMIC-IV spline

was approximately linear, the SYSU curve was J-shaped with a nadir near RAR 5.0. Despite this morphological difference, both cohorts converged on a clinically actionable threshold—mortality risk accelerated once RAR exceeded approximately 5.0–6.0, a range that aligns with previously reported cutoffs in sepsis and heart failure populations. Differences between cohorts may reflect heterogeneity in disease severity, treatment patterns, and baseline characteristics. The age-dependent interaction observed in MIMIC-IV ($P = 0.04$) may reflect the well-documented amplification of inflammatory and nutritional dysregulation in elderly CKD patients [24,25], rendering RAR a potentially more sensitive indicator in this subgroup. However, this interaction was not replicated in SYSU, possibly due to differences in age distribution or case-mix between the two populations.

The convergence of LASSO and Boruta on RAR—across two ethnically and geographically distinct cohorts—provides compelling evidence that RAR is a non-redundant predictor rather than an artifact of a single algorithm or population. Equally noteworthy is the finding that logistic regression matched or exceeded the discrimination of more complex models (AUC 0.758 vs. 0.777). This result echoes recent observations that, in moderately sized clinical datasets, regularized linear models often match ensemble methods while remaining far more transparent for clinical deployment [26].

Strengths and limitations of this study

- This is the first dual-center study to specifically examine the prognostic value of RAR in critically ill patients with concurrent hypertensive heart disease and CKD, with identical eligibility criteria applied across both cohorts.
- A triangulated analytic framework was used, combining multivariable regression, restricted cubic splines, two independent feature-selection algorithms (LASSO and Boruta), and SHAP interpretability.
- The retrospective design precludes causal inference, and residual confounding by unmeasured variables—particularly medication dosing and temporal trajectories of RDW and albumin—cannot be excluded.
- While multiple imputation assumes data are missing at random, the possibility of informative

missingness (e.g., sicker patients having more laboratory tests) cannot be entirely ruled out.

- The identified RAR thresholds require prospective validation before clinical implementation.

Future investigations might explore whether RAR retains its predictive edge when combined with dynamic inflammatory markers (e.g., neutrophil-to-lymphocyte ratio trajectories) or when incorporated into existing ICU mortality calculators as an augmentative variable [27–29].

Conclusions

In summary, this dual-center study establishes admission RAR as an independent, non-redundant predictor of in-hospital death among critically ill HP+CKD patients, with discriminative performance that exceeds either of its individual components and generalizes across geographically distinct populations. If prospectively validated, RAR could serve as a readily available bedside tool to enhance early risk stratification in this high-mortality subgroup.

List of abbreviations

ANN, artificial neural network; AUC, area under the curve; BUN, blood urea nitrogen; CI, confidence interval; CKD, chronic kidney disease; CRRT, continuous renal replacement therapy; DCA, decision curve analysis; GCS, Glasgow Coma Scale; HP+CKD, hypertensive heart disease with chronic kidney disease; ICU, intensive care unit; INR, international normalized ratio; IQR, interquartile range; LASSO, least absolute shrinkage and selection operator; LGB, LightGBM; LODS, Logistic Organ Dysfunction System; LR, logistic regression; MCHC, mean corpuscular haemoglobin concentration; MCV, mean corpuscular volume; MIMIC-IV, Medical Information Mart for Intensive Care IV; OASIS, Oxford Acute Severity of Illness Score; OR, odds ratio; PT, prothrombin time; PTT, partial thromboplastin time; RAR, red blood cell distribution width-to-albumin ratio; RBC, red blood cell; RCS, restricted cubic spline; RDW, red blood cell distribution width; ROC, receiver operating characteristic; SAPS II, Simplified Acute Physiology Score II; SD, standard deviation; SHAP, SHapley Additive exPlanations; SIRS, systemic inflammatory response syndrome; SOFA, Sequential Organ Failure Assessment; SVM, support vector machine; SYSU, Sun Yat-sen University; WBC, white blood cell; XGB, XGBoost.

Declarations

Ethics approval and consent to participate

This investigation adhered to the Declaration of Helsinki and followed the STROBE reporting checklist. Because MIMIC-IV contains only de-identified records, it is exempt from IRB review. The SYSU validation arm received ethics approval from the Institutional Review Board of the Third Affiliated Hospital of Sun Yat-sen University (approval number II2024-275-02), which granted a consent waiver given the anonymized, retrospective nature of the data. All data were anonymized and informed consent was waived.

Consent for publication

Not applicable.

Availability of data and materials

The MIMIC-IV data are available through PhysioNet (https://physionet.org/content/mimiciv/). The institutional validation cohort data cannot be publicly shared because of ethical restrictions; reasonable requests may be directed to the corresponding author.

Competing interests

The authors declare that they have no competing interests.

Funding

This work was supported by the Natural Science Foundation Project of Guangdong Basic and Applied

Basic Research Fund (Grant No. 2019A1515010969). The funder had no role in the study design, data collection, data analysis, data interpretation, or preparation of the manuscript.

Authors' contributions

FZ: Conceptualization, Methodology, Software, Formal analysis, Data curation, Writing — original draft. CJP: Methodology, Software, Formal analysis, Data curation, Writing — original draft. XX: Data curation, Investigation, Validation, Writing — review & editing. SM: Conceptualization, Methodology, Supervision, Project administration, Writing — review & editing. All authors read and approved the final manuscript and agree to be accountable for all aspects of the work.

Acknowledgements

We thank the staff of the Big Data Center of the Third Affiliated Hospital of Sun Yat-sen University for their assistance with data extraction and management, and the MIMIC-IV investigators for making the database publicly available.

References

1. Webster AC, Nagler EV, Morton RL, Masson P. Chronic kidney disease. Lancet. 2017;389:1238-52. https://doi.org/10.1016/S0140-6736(16)32064-5.

2. Duni A, Dounousi E, Pavlakou P, Eleftheriadis T, Liakopoulos V. Hypertension in chronic kidney disease: Novel insights. Curr Hypertens Rev. 2020;16:45-54. https://doi.org/10.2174/1573402115666190415153554.

3. Malhotra R, Kashani KB, Macedo E, Kim J, Bouchard J, Wynn S, et al. A risk prediction score for acute kidney injury in the intensive care unit. Nephrol Dial Transplant. 2017;32:814-22. https://doi.org/10.1093/ndt/gfx026.

4. Zhang Q, Fei Y, Jiang L. Risk factors for mortality in intensive care unit patients with sepsis combined with acute kidney injury after continuous renal replacement therapy: Secondary analysis of the data from a

multicenter observational study. Zhonghua Wei Zhong Bing Ji Jiu Yi Xue. 2019;31:155-9. https://doi.org/10.3760/cma.j.issn.2095-4352.2019.02.007.

5. Travers A, Farber HW, Sarnak MJ. Pulmonary hypertension in chronic kidney disease. Cardiol Clin. 2021;39:427-34. https://doi.org/10.1016/j.ccl.2021.04.004.

6. Reque J, Garcia-Prieto A, Linares T, Vega A, Abad S, Panizo N, et al. Pulmonary hypertension is associated with mortality and cardiovascular events in chronic kidney disease patients. Am J Nephrol. 2017;45:107-14. https://doi.org/10.1159/000453047.

7. He P, Hu JP, Li H, Tian XJ, He LJ, Sun SR, et al. Red blood cell distribution width and peritoneal dialysis-associated peritonitis prognosis. Ren Fail. 2020;42:613-21. https://doi.org/10.1080/0886022X.2020.1786401.

8. Lankinen R, Hakamäki M, Metsärinne K, Koivuviita NS, Pärkkä JP, Hellman T, et al. Cardiovascular determinants of mortality in advanced chronic kidney disease. Am J Nephrol. 2020;51:726-35. https://doi.org/10.1159/000509582.

9. Li J, Wang Y, Hao X, Jiang W. Association between red blood cell distribution width-to-albumin ratio and chronic kidney disease: A cross-sectional study. Medicine. 2026;105:e46980. https://doi.org/10.1097/MD.0000000000046980.

10. Kimura H, Tanaka K, Saito H, Iwasaki T, Kazama S, Shimabukuro M, et al. Impact of red blood cell distribution width-albumin ratio on prognosis of patients with CKD. Sci Rep. 2023;13:15774. https://doi.org/10.1038/s41598-023-42986-2.

11. Wang D, Zhu Z, Ren K, Duan X, Hu X, Lv Y, et al. Red cell distribution width-to-albumin ratio and chronic kidney disease mortality in adults: A population-based NHANES 1999 to 2020 study. Medicine. 2026;105:e44559. https://doi.org/10.1097/MD.0000000000044559.

12. Zhang T, Gao H, Wang S. The red cell distribution width to albumin ratio as a novel biomarker for predicting short-term mortality in severe pulmonary sepsis: A retrospective study with dual-cohort validation. Front Med. 2026;13:1805614. https://doi.org/10.3389/fmed.2026.1805614.

13. Yang H, Liang L, Liu Y, Wang X, Li J, Du X, et al. Prognostic significance of red cell distribution width to albumin ratio in ICU patients with non-alcoholic fatty liver disease: A retrospective analysis. BMC Gastroenterol. 2025;25:485. https://doi.org/10.1186/s12876-025-04019-2.

14. Pan LY, Song J. Association of red cell distribution width/albumin ratio and in-hospital mortality in patients with atrial fibrillation based on the MIMIC-IV database. BMC Cardiovasc Disord. 2024;24:174. https://doi.org/10.1186/s12872-024-03839-6.

15. Cai Y, Zhang Y, Zhou N, Tang Y, Zheng H, Liu H, et al. Association between red blood cell distribution width-to-albumin ratio and prognosis in post-cardiac arrest patients: Data from the MIMIC-IV database. Front Cardiovasc Med. 2024;11:1499324. https://doi.org/10.3389/fcvm.2024.1499324.

16. Li N, Li J, Wang K. Association between red blood cell distribution width-albumin ratio and all-cause mortality in intensive care unit patients with heart failure. Front Cardiovasc Med. 2025;12:1410339. https://doi.org/10.3389/fcvm.2025.1410339.

17. Aydın MK, Harput ZN, Tuncer MC. Red cell distribution width-to-albumin ratio as an early predictor of intensive care requirement and mortality in acute pancreatitis. Medicina. 2026;62:248. https://doi.org/10.3390/medicina62020248.

18. Chen X, Luo Y, Liu S. Association between red cell distribution width to albumin ratio and all-cause mortality in patients with acute pancreatitis admitted to the intensive care unit: A retrospective study based on the MIMIC-IV database. Front Med. 2025;12:1503378. https://doi.org/10.3389/fmed.2025.1503378.

19. Wang L, Cai Q. Value of red blood cell distribution width-to-platelet count ratio in predicting the prognosis of children with sepsis. Zhongguo Dang Dai Er Ke Za Zhi. 2019;21:1079-83.

20. Wei S, Xiaqin W, Liwei L, Fasu Z, Ying P, Pingping T, et al. Analysis of risk factors for death in the coronavirus disease 2019 (COVID-19) population: Data analysis from a large general hospital in Anhui, China. Cureus. 2024;16:e60069. https://doi.org/10.7759/cureus.60069.

21. Guo L, Chen D, Cheng B, Gong Y, Wang B. Prognostic value of the red blood cell distribution width-to-albumin ratio in critically ill older patients with acute kidney injury: A retrospective database study. Emerg Med Int. 2023;2023:3591243. https://doi.org/10.1155/2023/3591243.

22. Pan LN, Pan SA, Lei BH, Hong GL, Chen KW. Development of a novel nomogram incorporating red blood cell distribution width-albumin ratio for the prediction of 30-day mortality in acute pancreatitis patients. Emerg Med Int. 2022;2022:1573931. https://doi.org/10.1155/2022/1573931.

23. Tan MY, Zhang YJ, Zhu SX, Wu S, Zhang P, Gao M, et al. The prognostic significance of stress hyperglycemia ratio in evaluating all-cause and cardiovascular mortality risk among individuals across

stages 0-3 of cardiovascular-kidney-metabolic syndrome: Evidence from two cohort studies. Cardiovasc Diabetol. 2025;24:137. https://doi.org/10.1186/s12933-025-02689-6.

24. Kari JA, Desoky SME, Farag YM, Singh AK. Predictors of renal replacement therapy and mortality in children with chronic kidney disease. Saudi Med J. 2015;36:32-9. https://doi.org/10.15537/smj.2015.1.9774.

25. Mohamed NE, Benn EKT, Astha V, Okhawere KE, Korn TG, Nkemdirim W, et al. Association between chronic kidney disease and COVID-19-related mortality in New York. World J Urol. 2021;39:2987-93. https://doi.org/10.1007/s00345-020-03567-4.

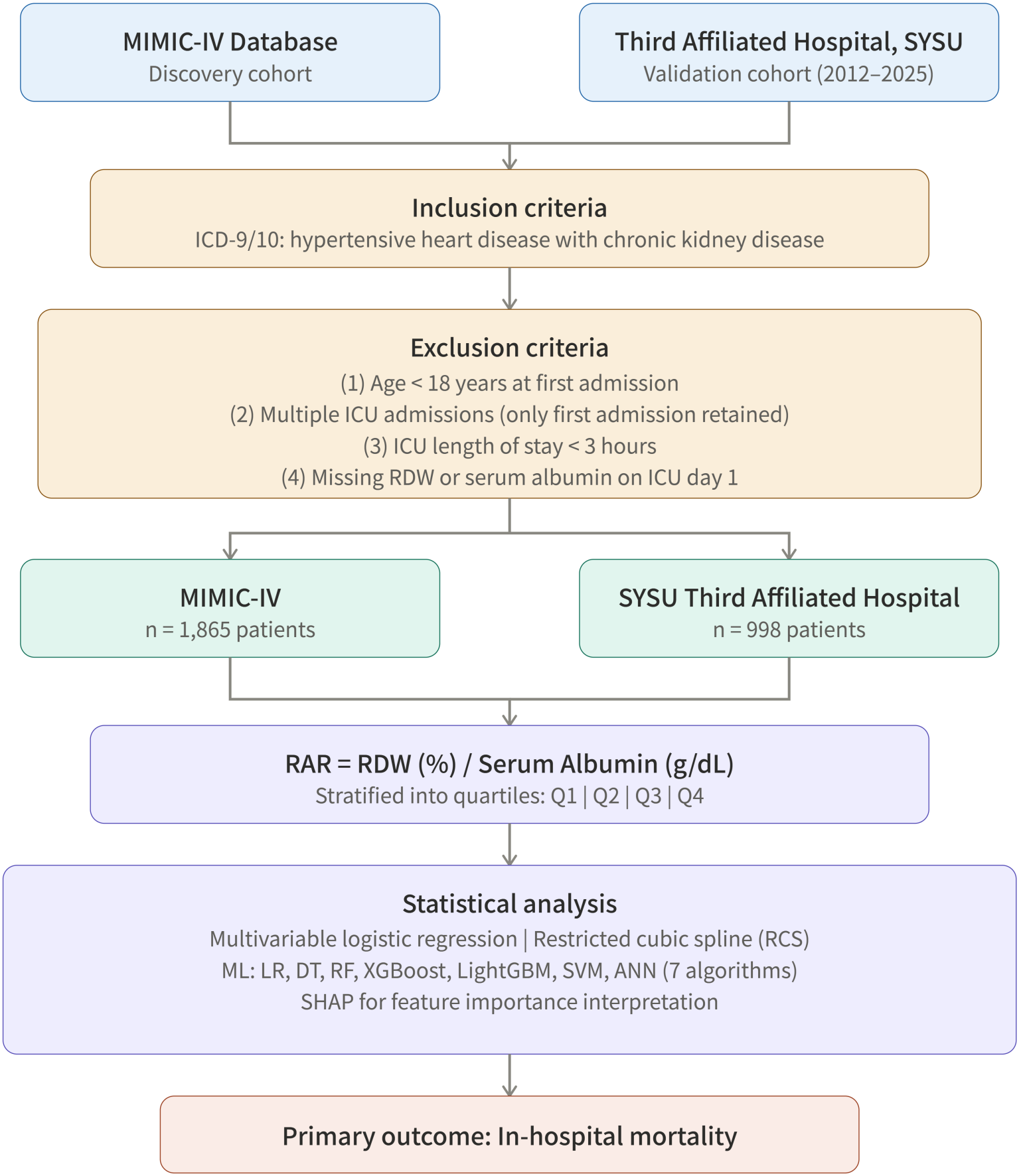
26. Li H, Xu Y. Association between red blood cell distribution width-to-albumin ratio and prognosis of patients with acute myocardial infarction. BMC Cardiovasc Disord. 2023;23:66. https://doi.org/10.1186/s12872-023-03094-1.

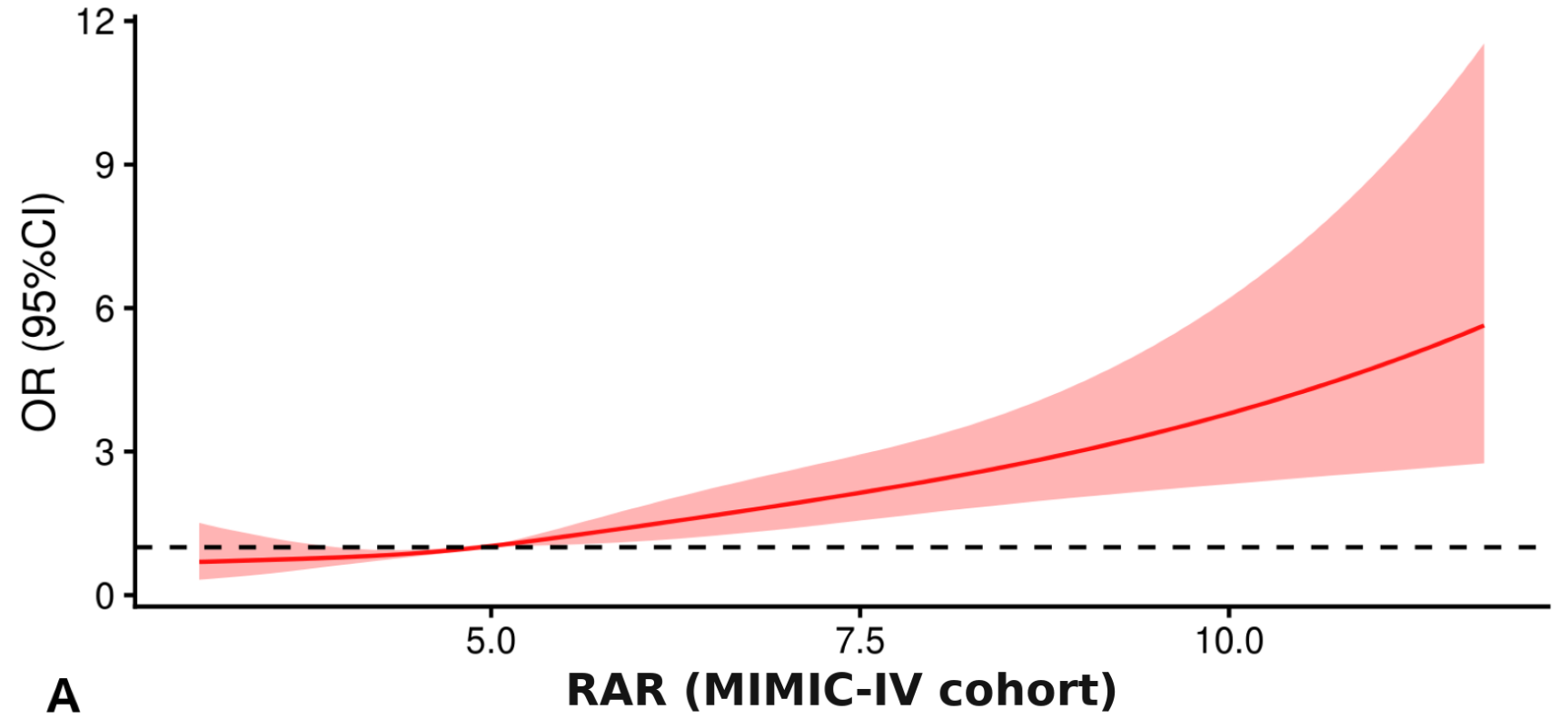
27. You W. Roles of cytokine storm in sepsis progression: Biomarkers, and emerging therapeutic strategies. Front Immunol. 2025;16:1696366. https://doi.org/10.3389/fimmu.2025.1696366.

28. Santos RSS, Motwani SS, Elias RM. Chronic kidney disease and sleeping disordered breathing (SDB). Curr Hypertens Rev. 2016;12:43-7. https://doi.org/10.2174/1573402112666160114094222.

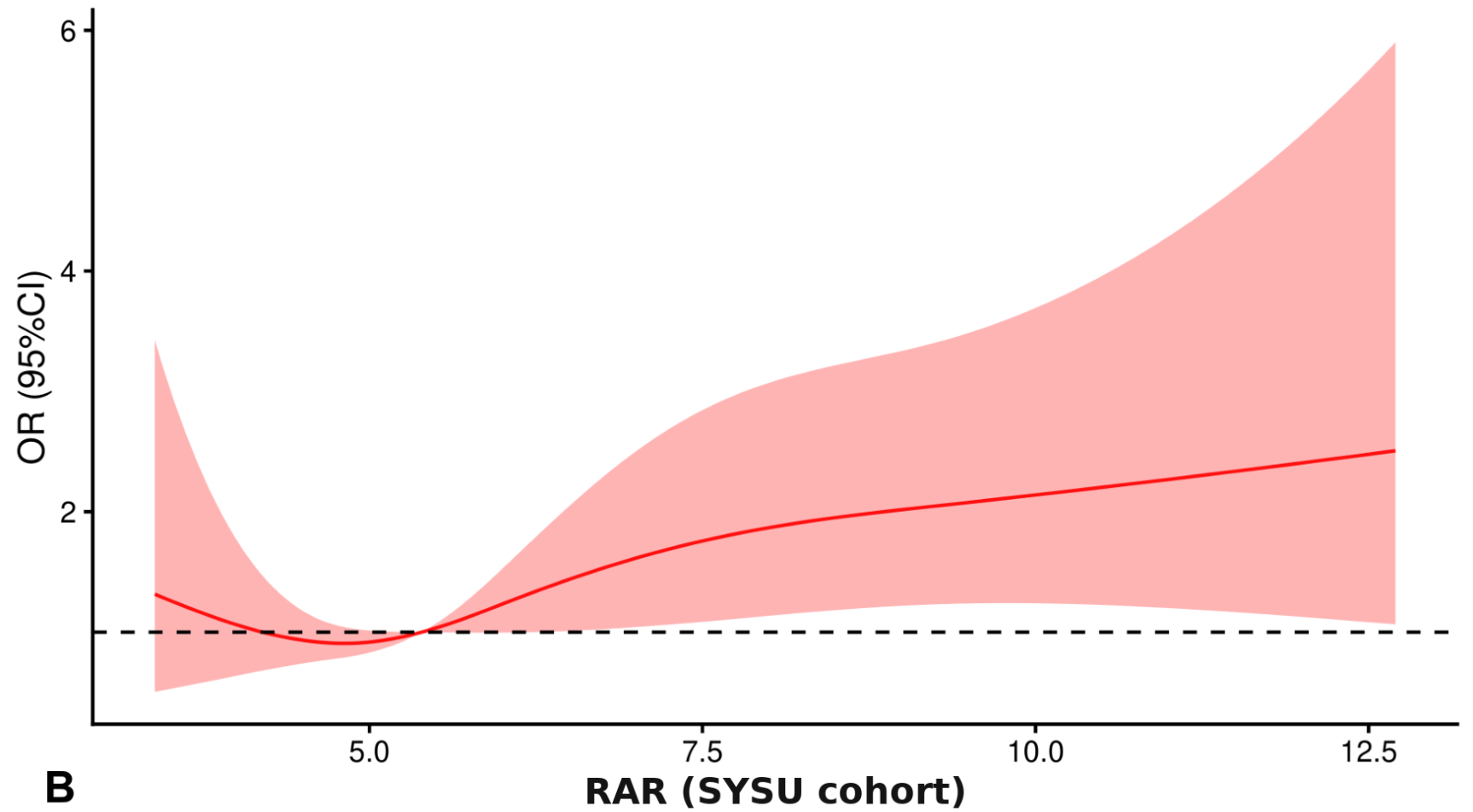
29. Goudis C, Daios S, Korantzopoulos P, Liu T. Does CHA2DS2-VASc score predict mortality in chronic kidney disease? Intern Emerg Med. 2021;16:1737-42. https://doi.org/10.1007/s11739-021-02799-5.

Study Design: RAR and In-hospital Mortality in Critically Ill HP+CKD Patients



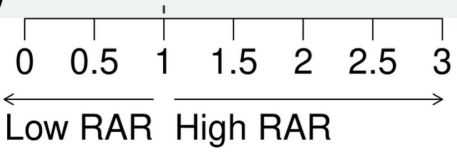

12
9
6
3
0
OR (95%CI)
5.0
7.5
10.0
RAR (MIMIC-IV cohort)

A


6
4
2
OR (95%CI)
5.0
7.5
10.0
12.5
RAR (SYSU cohort)

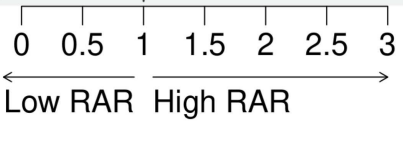
B

Variables	OR(95%CI)	P for interaction
Overall	1.3(1.2–1.41)	
Age		0.04
>65	1.77(1.38–2.27)	
=65	1.26(1.16–1.37)	
Gender		0.3
Male	1.35(1.22–1.51)	
Female	1.25(1.1–1.42)	
Race		0.64
Others	1.31(1.15–1.5)	
White	1.3(1.17–1.44)	
Dobutamine		0.15
YES	1.34(1.23–1.46)	
NO	1.01(0.72–1.41)	
Norepinephrine		0.09
YES	1.36(1.23–1.51)	
NO	1.22(1.07–1.38)	
CRRT Flag		0.93
NO	1.3(1.19–1.41)	
YES	1.36(1.05–1.76)	

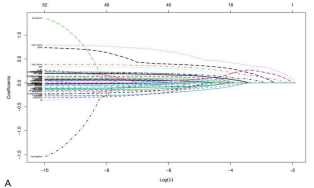


A

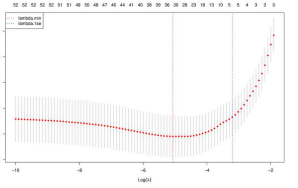
Variables	OR(95%CI)	P for interaction
Overall	1.14(1.03–1.25)	
Age		0.71
>65	1.19(1–1.42)	
=65	1.12(0.99–1.27)	
gender		0.49
Male	1.19(1.01–1.4)	
Female	1.14(1–1.3)	
norepinephrine		0.14
NO	1.16(1.05–1.29)	
YES	1.25(0.63–2.47)	
ventilation_flag		0.16
NO	1.2(1.04–1.39)	
YES	1.12(0.98–1.28)	



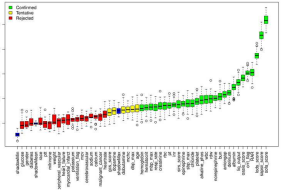
B


Coefficients
Log(λ)

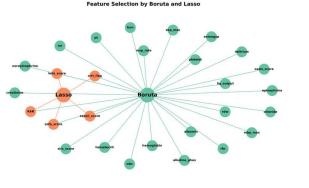
A


lambda.min
lambda.1se
Binomial Deviance
Log(λ)

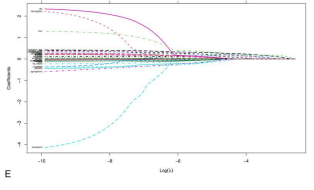
B


Confirmed
Tentative
Rejected
Importance

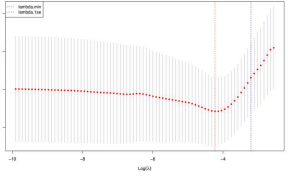
C


Feature Selection by Boruta and Lasso
Lasso
Boruta

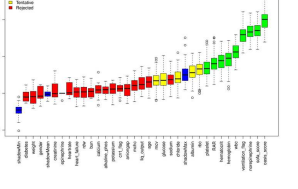
D


Coefficients
Log(λ)

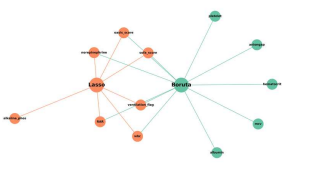
E


lambda.min
lambda.1se
Binomial Deviance
Log(λ)

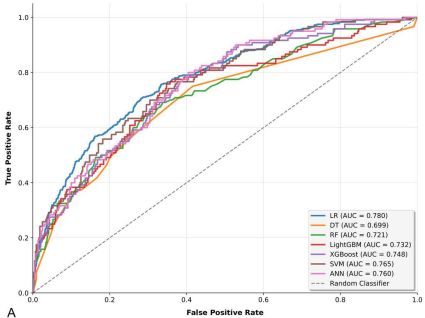
F


Confirmed
Tentative
Rejected
Importance

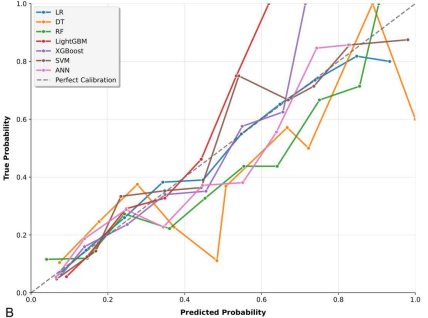
G


Feature Selection by Boruta and Lasso
Lasso
Boruta

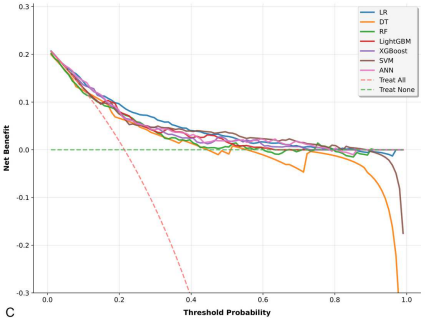
H


ROC Curves (Training set)
True Positive Rate
False Positive Rate
LR (AUC = 0.780)
DT (AUC = 0.699)
RF (AUC = 0.721)
LightGBM (AUC = 0.732)
XGBoost (AUC = 0.748)
SVM (AUC = 0.765)
ANN (AUC = 0.760)
Random Classifier

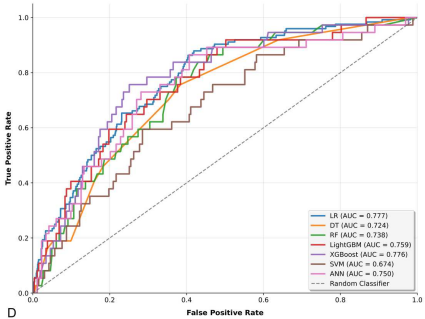
A


Calibration Curves (Training set)
True Probability
Predicted Probability
LR
DT
RF
LightGBM
XGBoost
SVM
ANN
Perfect Calibration

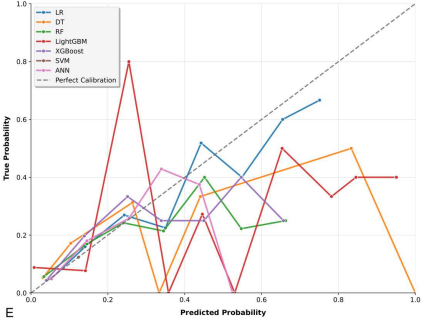
B


Decision Curve Analysis (Training set)
Net Benefit
Threshold Probability
LR
DT
RF
LightGBM
XGBoost
SVM
ANN
Treat All
Treat None

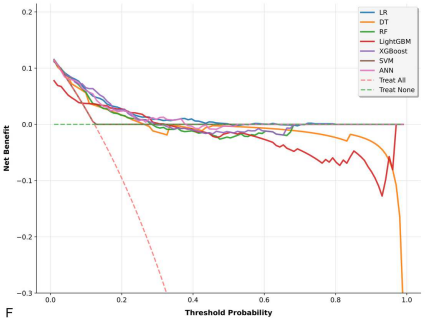
C


ROC Curves (Training set)
True Positive Rate
False Positive Rate
LR (AUC = 0.777)
DT (AUC = 0.724)
RF (AUC = 0.738)
LightGBM (AUC = 0.759)
XGBoost (AUC = 0.776)
SVM (AUC = 0.674)
ANN (AUC = 0.750)
Random Classifier

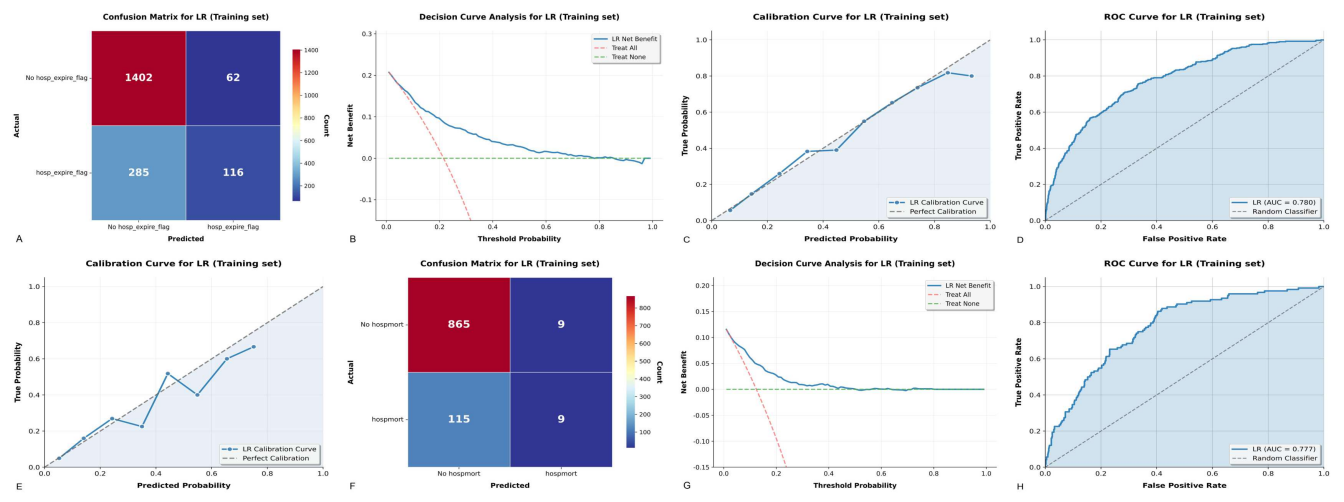
D

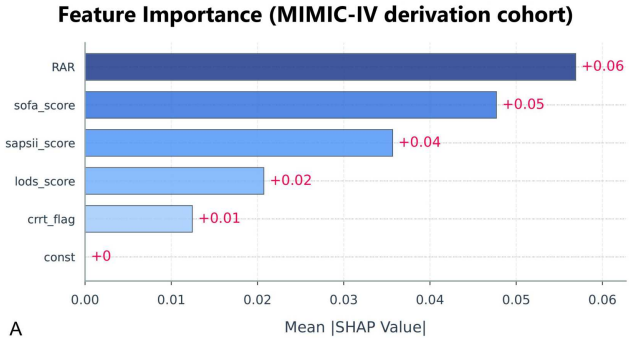

Calibration Curves (Training set)
True Probability
Predicted Probability
LR
DT
RF
LightGBM
XGBoost
SVM
ANN
Perfect Calibration

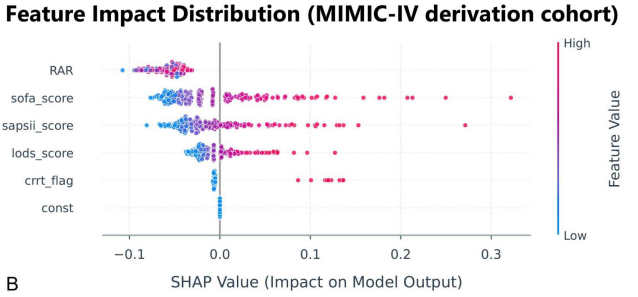
E

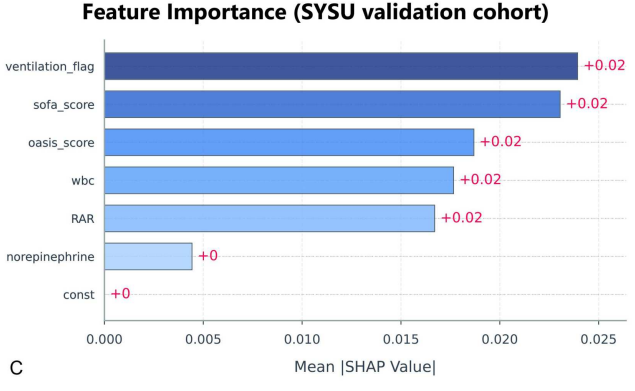

Decision Curve Analysis (Training set)
Net Benefit
Threshold Probability
LR
DT
RF
LightGBM
XGBoost
SVM
ANN
Treat All
Treat None

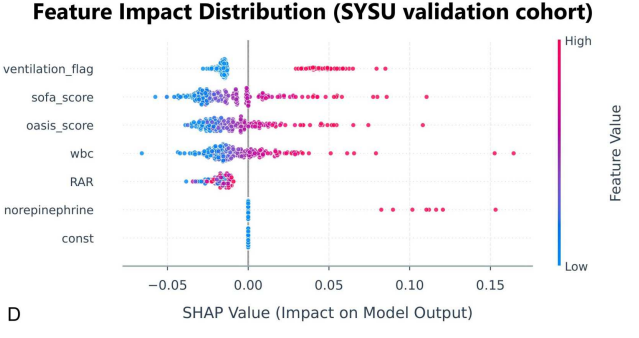
F


Confusion Matrix for LR (Training set)
No hosp_expire_flag
hosp_expire_flag
Actual
1402
62
285
116
Count
1400
1200
1000
800
600
400
200
No hosp_expire_flag
hosp_expire_flag
Predicted
A
Decision Curve Analysis for LR (Training set)
LR Net Benefit
Treat All
Treat None
Net Benefit
Threshold Probability
B
Calibration Curve for LR (Training set)
True Probability
LR Calibration Curve
Perfect Calibration
Predicted Probability
C
ROC Curve for LR (Training set)
True Positive Rate
LR (AUC = 0.780)
Random Classifier
False Positive Rate
D
Calibration Curve for LR (Training set)
True Probability
LR Calibration Curve
Perfect Calibration
Predicted Probability
E
Confusion Matrix for LR (Training set)
No hospmort
hospmort
Actual
865
9
115
9
Count
800
700
600
500
400
300
200
100
No hospmort
hospmort
Predicted
F
Decision Curve Analysis for LR (Training set)
LR Net Benefit
Treat All
Treat None
Net Benefit
Threshold Probability
G
ROC Curve for LR (Training set)
True Positive Rate
LR (AUC = 0.777)
Random Classifier
False Positive Rate
H


Feature Importance (MIMIC-IV derivation cohort)
RAR
sofa_score
sapsii_score
lods_score
crrt_flag
const
+0.06
+0.05
+0.04
+0.02
+0.01
+0
0.00
0.01
0.02
0.03
0.04
0.05
0.06
Mean |SHAP Value|
A


Feature Impact Distribution (MIMIC-IV derivation cohort)
RAR
sofa_score
sapsii_score
lods_score
crrt_flag
const
−0.1
0.0
0.1
0.2
0.3
SHAP Value (Impact on Model Output)
High
Low
Feature Value
B


Feature Importance (SYSU validation cohort)
ventilation_flag
sofa_score
oasis_score
wbc
RAR
norepinephrine
const
+0.02
+0.02
+0.02
+0.02
+0.02
+0
+0
0.000
0.005
0.010
0.015
0.020
0.025
Mean |SHAP Value|
C


Feature Impact Distribution (SYSU validation cohort)
ventilation_flag
sofa_score
oasis_score
wbc
RAR
norepinephrine
const
−0.05
0.00
0.05
0.10
0.15
SHAP Value (Impact on Model Output)
High
Low
Feature Value
D